SERS characterization of aggregated and isolated bacteria deposited on silver-based substrates

Cristina-Cassiana Andrei,[a] Anne Moraillon,[a] Eric Larquet,[a] Monica Potara,[b] Simion Astilean,[b,c] Endre Jakab,[d,e] Julie Bouckaert,[f] Léa Rosselle,[g,h] Nadia Skandrani,[g] Rabah Boukherroub,[h] François Ozanam,[a] Sabine Szunerits,[h,] Anne Chantal Gouget-Laemmel[a,*]*

[a]Laboratoire de Physique de la Matière Condensée, Ecole Polytechnique, CNRS, IP Paris, 91128 Palaiseau, France

[b]Nanobiophotonics and Laser Microspectroscopy Center, Interdisciplinary Research Institute in Bio-Nano-Sciences, Babes-Bolyai University, T. Laurian Str. 42, 400271, Cluj-Napoca, Romania

[c]Department of Biomolecular Physics, Faculty of Physics, Babes-Bolyai University, M Kogalniceanu Str. 1, 400084, Cluj-Napoca, Romania

[d]Hungarian Department of Biology and Ecology, Faculty of Biology and Geology, Babes-Bolyai University, Clinicilor 5-7, 400006 Cluj-Napoca, Romania

[e]Molecular Biology Center, Interdisciplinary Research Institute in Bio-Nano-Sciences, Babes-Bolyai University, T. Laurian Str. 42, 400271, Cluj-Napoca, Romania

[f]Unité de Glycobiologie Structurale et Fonctionnelle (UGSF), UMR 8576 of the CNRS and the Univ. Lille, 50 avenue de Halley, 59658 Villeneuve d'Ascq, France

[g]TissueAegis SAS, 14E rue Pierre de Coubertin, 21000 Dijon

[h]Univ. Lille, CNRS, Centrale Lille, Univ. Polytechnique Hauts-de-France, UMR 8520-IEMN, F-59000 Lille, France.

Corresponding authors : sabine.szunerits@univ-lille.fr and anne-chantal.gouget@polytechnique.edu

Abstract

Surface-enhanced Raman scattering (SERS), based on the enhancement of the Raman signal of molecules positioned within a few nanometres from a structured metal surface, is ideally suited to provide bacterial specific molecular fingerprints which can be used for analytical purposes. However, for some complex structures such as bacteria, the generation of reproducible SERS spectra is still a challenging task. Among the various factors influencing the SERS variability (such as the nature of SERS active substrate, Raman parameters and bacterial specificity), we demonstrate in this study that the environment of Gram-positive and Gram-negative bacteria deposited on ultra-thin silver film also impacts the origin of the SERS spectra. In the case of densely packed bacteria, the obtained SERS signatures were either characteristic of the secretion of adenosine triphosphate for *Staphylococcus aureus* (*S. aureus*) or the cell wall and the pili/flagella for *Escherichia coli* (*E. coli*), allowing for an easy discrimination between the various strains. In the case of isolated bacteria, SERS mapping together with Principal Component Analysis revealed some variabilities of the spectra as a function of the bacteria environment and the bactericidal effect of the silver. However, the variability does not preclude the SERS signatures of various *E. coli* strains to be discriminated.

Keywords: Surface-Enhanced Raman Scattering (SERS); silver nanostructures; *Escherichia coli*; *Staphylococcus aureus*; aggregated and single bacteria, Principal Component Analysis (PCA).

1. Introduction

Rapid and reliable identification of pathogenic bacteria is a great challenge in many fields such as health care, food and environmental safety or bioterrorism prevention. Nowadays, the marketed standardized detection systems are mainly based on bacteriological culture and colouring methods using selective media, which are labour and time-consuming [1],[2]. As an example, the detection of *Listeria monocytogenes* in food (ISO 11290-1:2017) requires at least four days. Although various other methods based on polymerase chain reaction (PCR) [3], immunological-related techniques [4] or mass spectrometry [5] have emerged over the years to alleviate the detection speed problem, they all require extensive sample preparation procedure and high technical knowledge. A much shorter diagnosis time with minimum requirement for sample handling is desirable to meet safety and the establishment of fast actions of decontamination in order to prevent or avoid epidemic risks related to a specific pathogenic agent. In such a context, Surface-Enhanced Raman Spectroscopy (SERS) is a promising solution since it offers a simple and fast identification of the specific spectral fingerprint of bacteria with good sensitivity in aqueous media without interference from water bands [6]. Moreover, this technique is non-destructive and reagentless, without the need of prior labelling, and has the potential to be used *on the spot*, thanks to commercially available portable devices. The SERS process relies on the Raman signal enhancement of bacteria adsorbed on or in close vicinity of metallic nanostructures due to the strong electromagnetic field generated by the excitation of localized surface plasmons. To obtain SERS effect of bacteria without any labels or reporters, two main strategies have been developed [7]. The first one relies on the direct interaction of gold or silver colloidal nanoparticles with bacteria [8],[9],[10]. The second one is the direct bacteria identification by placing them on SERS-

active solid substrates, which can be prepared by a variety of techniques [11],[12],[13], generating hot spots responsible for high local electromagnetic field enhancement [14],[15]. For this study, we have chosen the simplest technique, i.e. thermal evaporation [16]-[17], which has successfully been used for the preparation of reproducible SERS substrates mainly for the detection of dyes [18],[19] and biomolecules [20],[21]. Concerning the characterization of microorganisms, up to now, there are a very few examples reported on the use of such easy-to-produce SERS substrates obtained by direct thermal evaporation on glass [22], [23].

A major challenge concerns the variability of the SERS spectra of the analysed bacteria and the origin of the vibrations [24]. In contrast to small analytes, which are in intimate contact with the SERS-active metal nanostructures, a good reproducibility of the SERS signal of large structures such as bacteria is often difficult to achieve. These fluctuations can be explained by several factors: uncontrolled or inhomogeneous binding between the substrate and the bacteria, stability of the bacterial sample under Raman excitation [25],[26], the growth procedure and sample preparation, leading to differences in chemical information [27]. To overcome these limitations, multivariate statistical-based analysis is often coupled with SERS spectroscopy in order to extract the relevant characteristic features of bacteria and to establish classification and discrimination between strains [9],[28],[29].

In this work, we focus on another parameter/factor which has not been considered yet, the influence of the bacteria environment on the SERS response/variability. The Raman analysis of aggregated (densely packed bacteria) and single bacteria, in close contact with silver surface, has been investigated using two types of bacteria Gram-positive *Staphylococcus aureus* (*S. aureus*) and Gram-negative *Escherichia coli* (*E. coli*). We have used ultra-thin silver films deposited on glass substrate by thermal evaporation, providing excellent SERS reproducibility and transparency, allowing for an easy localization of the densely packed or

isolated bacteria under the laser beam. We chose silver thin film instead of gold thin films because of their higher SERS performances [30],[31]. A special effort has been devoted to characterize the SERS spectra of five different strains. Additionally, Principal Component Analysis (PCA) has been applied to measure the statistical variability of the SERS response as a function of the bacteria aggregation.

2. Experimental section

2.1. Materials

All chemicals were used as-received. ß-Nicotinamide adenine dinucleotide (NADH), uric acid, adenine and adenosine, adenosine mono-, di- and triphosphate (AMP, ADP, ATP, respectively) were purchased from Sigma-Aldrich. Rhodamine B (RhB) was obtained from Fluka. Hydrogen peroxide (H_2O_2, 30%), sulfuric acid (H_2SO_4, 96%) and anhydrous ethanol were of RSE grade and supplied by Carlo Erba. Ultrapure water (Milli-Q, 18 MΩ cm^{-1}) was used as solvent and for all rinses. *S. aureus* 43300 strain used for SEM imaging was kindly provided by the CHU Lille. *S. aureus* ATCC 25923 strain used for SERS measurements was purchased from LGC Standards Gmbh, Wesel, Germany. *E. coli* JM101TR was obtained from the biochemistry laboratory (BIOC) at Ecole Polytechnique (France) [32]-[33]. *E. coli* Katushka was produced by the transformation of *E. coli* K12 MG1655 (ATCC 700926) with the pDONR221-nadB-cat recombinant plasmid [34]. *E. coli* pUT2002 strain is the AAEC185 mutant strain that does not express type 1 fimbriae and was transformed with the pUT2002 plasmid that encodes the entire *fim* cluster, except the gene coding for the adhesin *fimH* [35].

2.2. Preparation of the SERS substrates

Microscope glass slides were used as substrates for the deposition of silver layers. They were first copiously rinsed with water then with TFD4 type detergent (Franklab), before being

immersed in absolute ethanol for 15 min. After vigorously rinsing with deionized water, the slides were further immerged into a piranha solution (1/3 H_2O_2/H_2SO_4; caution: very corrosive) for 15 min. After a final rinse with ultrapure Milli-Q water and drying under nitrogen flow, silver thin films were deposited using a home-made thermal evaporator as follows: a 10 cm long silver wire (99.99% purity, 0.25 mm diameter, supplied by Goodfellow) was deposited on a tungsten crucible, which was heated up under vacuum. The deposition was made under a pressure of 25-35 10^{-6} Torr. The reproducibility of the Ag evaporation was evaluated by measuring the LSPR signals of 4-6 samples after each deposition batch. The standard deviation in the wavelength (λ_{max}) is typically 2 nm.

Four different thicknesses of 4, 5, 7 and 9 nm were deposited. Their preparation, characterization and their optimization for dye probes detection were described in Electronic Supplementary Material, **section S1**. We found that the 7 nm-thick Ag films gave the highest SERS enhancement for rhodamine B and crystal violet with excellent reproducibility. It also displayed a remarkable stability over time (no significant change of the plasmon band after 4 months storage under vacuum and one year in air). Therefore, such 7 nm-thick Ag film was chosen for the study of bacteria.

2.3. Characterization

UV/Vis spectrometer

Absorption spectra were recorded using a Cary300 UV-Vis spectrophotometer. The wavelength range was 200-800 nm.

Raman measurements

For recording SERS spectra of analytes (rhodamine B, crystal violet, biomolecules and metabolites) or bacteria in solution, droplets of ~3 µL were directly deposited onto the SERS substrates and Raman measurements were performed after 30 min when all the droplets are

dried. Glass slides were used as control to check that the response of the bacteria/(bio)molecules is a SERS effect and not a Raman effect by using the same experimental parameters as for SERS measurements. The focus of the laser on the sample was made through an optical camera. Using 10× lens first, then 50× and finally 100×, the focus was adjusted until a clear image was obtained.

A confocal Raman microscope (CRM alpha 300R from WITec GmbH, Germany) was used to perform the SERS measurements on *S. aureus*. The samples were excited using the 633 nm line of a He-Ne laser. The Raman backscattered light collected through the objective (100×, NA=0.9) was passed through a holographic edge filter, before being focused into a multimode optical fibre of 100 µm diameter, which provides the optical pinhole for confocal measurement. The light emerging from the output optical fibre was analysed by a f/4 300 mm focal length ultrahigh throughput spectrometer (UHTS 300 incorporating interchangeable gratings) equipped with back-illuminated deep-depletion 1024 × 128 pixel CCD camera (DV_{401}-BV, Andor) operating at -60 °C. We used a 600 grooves/mm grating blazed at 500 nm that delivers approximatively 2 cm^{-1} spectral resolution. Since the slit width is set to 100 µm (actually the pinhole), a practical resolution of ~ 8 cm^{-1} is found. The measurements were conducted by choosing an integration time of 10 s for each spectrum and a laser power incident on the samples of 2.5 mW. The reproducibility of SERS measurements was investigated by recording several spectra from different spots across a particular substrate. The distance between the measured spots in the SERS experiments varies from 2.3 µm to 33.4 µm. The Raman spectrum of *S. aureus* (10^9 CFU mL^{-1}) was recorded from a dried droplet deposited on a glass slide using the same experimental parameters as for SERS measurements. The WITec Project Four Plus software was used for spectral analysis. Reflected-light bright-field optical images were captured with a colour video camera attached

to the eyepiece output of the same microscope using for illumination a super-bright white LED source.

The instrument Horiba/Jobin Yvon LabRam HR equipped with a laser emitting at 633 nm was used for SERS measurements of *E. coli* strains and the (bio)chemicals (dyes and metabolites). The ultimate resolution of the spectrometer with a grating of 1800 gr/mm is 0.3 cm^{-1}, leading to a spectral resolution of ~1.8 cm^{-1}. The spectra were recorded in the 200-2200 cm^{-1} range using a 100× objective (NA=0.95) at different incident laser powers (0.1, 0.5, 1 and 2.5 mW) in order to avoid the photo-degradation of the samples and spectral data acquisition times from 10 to 30 s. The grating used was 300 gr/mm with a slit width set to 100 µm, yielding a practical resolution of ~8 cm^{-1}. The spectra were analysed with Labspec6 and the 521 cm^{-1} band of a silicon wafer was used for frequency calibration. Spectra were baseline-corrected and normalized for display. The mappings of single bacteria obtained from the deposit of *E. coli* JM101TR strains at 10^4 CFU mL^{-1} (mapping 1), at 10^8 CFU mL^{-1} (mapping 2) and of group of bacteria obtained from the deposit of 10^9 CFU mL^{-1} (mapping 3) were collected by choosing rectangular areas of 6 µm × 7 µm (mapping 1), 3.5 µm × 4.5 µm (mapping 2) and 3.5 µm × 4.5 µm (mapping 3). The mappings are composed of typically about 20-30 measurement points. Spectra were collected at each 0.6 µm. This step was chosen higher than the diameter of the laser spot (~0.35 µm), in order to avoid multiple acquisitions in the same spot, thus to avoid the local photodegradation.

Scanning electron microscopy (SEM)

SEM images of silver substrates and *E. coli* bacteria deposited on the silver substrates were recorded using a SEM Hitachi 4800 microscope operating at 3 to 5 kV. Samples were fixed with 1% glutaraldehyde solution for 30 min in the dark at room temperature. For a better contrast, the samples containing bacteria were coated with a very thin platinum layer before

scanning. SEM images of *S. aureus* were obtained using a Zeiss Merlin VP compact electron microscope at 1 kV under high vacuum (Zeiss, France).

2.4. SERS measurements of metabolites

Solutions of different metabolites (18.5 mM) were prepared in acidic or basic solutions in order to ensure their dissolution as follows: adenine was dissolved in 5 % CH_3COOH, uric acid and adenosine in 0.5 mM NaOH aqueous solution, and AMP, ADP, ATP and NADH in pure Milli-Q water. Droplets of 3 µL were deposited onto the SERS substrates (7 nm-thick Ag film) and after 30 min when the droplets are dried, Raman measurements were recorded using 633 nm laser at 0.1 mW, 100× objective, 10 s acquisition time for each spectrum.

2.5. Bacterial growth conditions

The well-characterized *S. aureus* strain (ATCC 25923) was cultured overnight in a shaking incubator (ES 20/60, Biosan, Riga, Latvia) in Mueller-Hinton broth at 37ºC and 200 rpm until the light absorbance at 600 nm reached 1.0 (corresponding to 10^9 cfu mL^{-1} – Spekol UV VIS 3.02, Analytic Jena, Jena, Germany). The bacterial suspension was pelleted at 5000 × g for 10 min at 20ºC then washed three times with ultrapure water (Purelab Ultra Genetic, ELGA LabWater, High Wycombe, UK). After that, a ten-fold dilution series was prepared using ultrapure water. *S. aureus* strain (ATCC 43300 used for SEM imaging) was grown in Brain Heart Infusion (BHI) broth at 37°C with shaking until the OD_{600} reached 0.5-1. The *E. coli* JM101TR and Katushka strains were grown in 2× YT medium. This nutrient-rich microbial broth is composed of 16 g/L Tryptone, 10 g/L Yeast Extract and 5.0 g/L NaCl at pH ~6.8. The AAEC185 (pUT2002) and AAAEC185 (pMMB66) strains were grown in LB medium with antibiotic selection (25 µg/mL chloramphenicol for pUT2002 and 100 µg/mL ampicillin for pMMB66). In all cases, the growth was done at 37°C with shaking until the OD_{600} reached

0.5-1. Part of the culture (10 mL) was washed with ultrapure Milli-Q water (20 mL), re-suspended in Milli-Q water (1 mL) and diluted to required concentration.

2.6. Principal component analyses (PCA)

PCA was performed with Origin Pro software. The spectral region from 200 to 2200 cm^{-1} was taken into-account. The order of the principal components indicates their importance to the datasets. By maximizing the variance, PC1 describes the spectral weighting which maximizes the discrimination among the various data sets, PC2, by maximizing the residual variance describes a weighting that maximizes the discrimination in a subset orthogonal to PC1, and so on. The percentages associated to each principal component indicate the respective contribution of each component to the total variance (i.e., their relevance in the discrimination process). In the PCA analysis, all the spectra presented in this work were taken into account (3 to 5 per strain) as they were obtained on the SERS study: *E. coli* JM101TR (low concentration), *S. aureus* (high and low concentrations) together with supplementary spectra (where more spectra were acquired) in the case of *E. coli* PMMB66 (11 spectra), *E. coli* Katushka (6 spectra).

3. Results and discussion

3.1. SERS signature of densely packed bacteria on glass/Ag NSs surfaces

Two model bacteria were directly deposited on the SERS active 7 nm-thick Ag substrate: the Gram-positive *S. aureus* and Gram-negative *E. coli*. They are expected to strongly interact with Ag NSs since both of them have a negatively charged cell wall due to the presence of teichoic acids for *S. aureus* and phosphoryl and carboxylate groups in lipopolysaccharides for *E. coli* [36]. In a first stage, we focused on the SERS response of a homogeneous and dense layer of bacteria on top of the Ag substrate. In order to obtain such a layer, high

concentrations of bacteria are necessary, as depicted in the optical images in Electronic Supplementary Material **Figure S2-1**, with values $\geq 10^8$ CFU mL^{-1} for *S. aureus* and 10^{10} CFU mL^{-1} for *E. coli*. SEM images (**Figure 1**) reveal the formation of densely-packed bacteria carpets for *S. aureus,* whereas large domains of interlinked bacteria together with small areas of naked Ag substrate are observed for *E. coli*. In both cases, the spherical shape for *S. aureus* and the rod-like shape for *E. coli* are preserved.

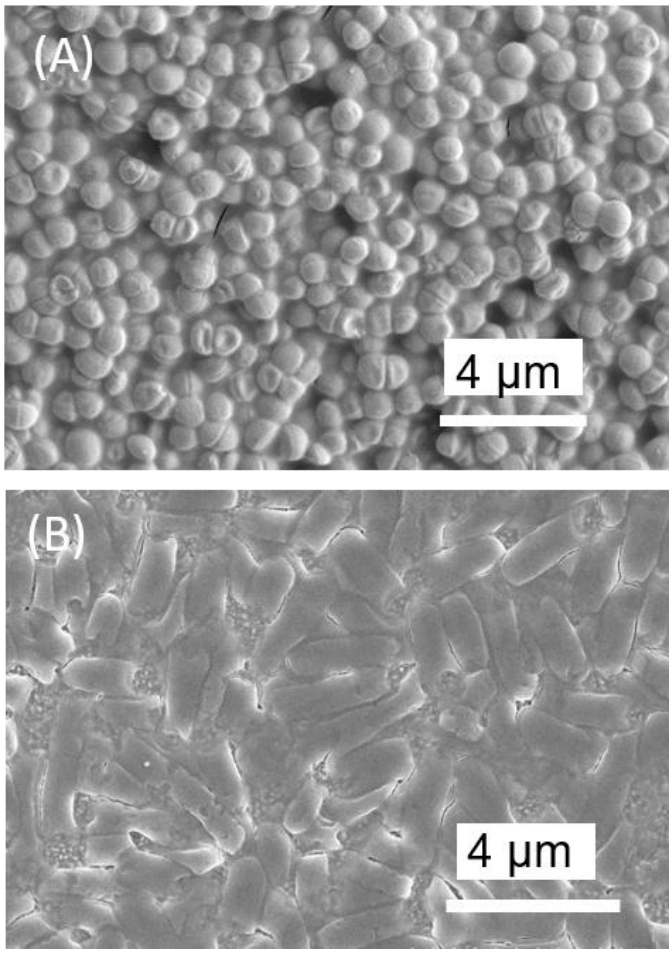

Figure 1. SEM images of (A) *S. aureus* ATCC 43300 deposited at 10^8 CFU mL^{-1} and (B) *E. coli* JM101TR deposited at 10^{10} CFU mL^{-1} on the 7 nm-thick Ag substrate.

SERS spectra of *S. aureus* ATCC 25923 strain were first measured at 633 nm on random places (**Figure 2**) and show very high reproducibility with an intense vibration band located at 231 cm^{-1} due to silver-oxide mode or ionic species sorbed onto the metal surface [37]. No SERS response was recorded from the substrate itself (in absence of bacteria) or when the bacteria were directly deposited on glass. Surprisingly, their spectral fingerprints appear to consist of a restricted number of peaks. It is well-accepted that only cell wall components in close vicinity to the SERS substrate, within approximately 10 nm, contribute to the SERS signal [38],[39],[40]. In our case, two bands at 730 and 1323 cm^{-1} are mainly observable and are characteristic of adenine vibrations, more precisely ascribed to the ring breathing mode, and δ(C-H, N-H) bending and ν(C-N) stretching modes of the adenine ring, respectively. Contributions from the aromatic rings are also visible at 1397 and 1457 cm^{-1} [41],[21], confirming the presence of adenine/adenosine type compounds. When bacteria are placed directly onto a SERS-active substrate, it has been demonstrated that dominant molecular species arise essentially from metabolites secreted by the bacteria [7],[42] or from a bacterial lysis [43]. From these considerations and from the SERS spectra of adenine-related compounds recorded on the 7 nm-thick Ag substrate (see **Figure S2-2**), we deduce that the signature of *S. aureus* is dominated by the signature of adenosine and/or adenosine triphosphate (ATP) since they have similar signatures. Close examination of the spectra reveals a better coincidence of the *S. aureus* Raman features with those of ATP rather with those of adenosine, even though the intensity ratio of the main bands would better match with adenosine. Indeed, the overlap between the SERS spectra of ATP and *S. aureus* is optimal in the 1460-1800 cm^{-1} and 900-925 cm^{-1} spectral regions (**Figure S2-2B-C**). For adenosine, there are additional peaks at 908 cm^{-1} and at wavenumbers higher than 1450 cm^{-1}, as compared to ATP and *S. aureus*. The band at 1125 cm^{-1} may be associated to the stretching mode of phosphate groups [44]. No evidence of DNA/RNA species is found since the

signatures of the bases at around 700-800 cm^{-1} and above 1600 cm^{-1} are absent [45],[46]. Notably, the absence of a peak at 652 cm^{-1} characteristic of DNA bases (i.e. guanine and thymine bases) disfavors the alternative possibility of bacterial genome release, as mentioned in the work of Lemma *et al*. [47]. In addition, bacterial cells are known to secrete extracellular ATP during growth [48] or when exposed to a surface [49],[50],[51]. Although hydrolysis or degradation of ATP into purine components like adenosine has been reported [42],[48], to our knowledge, no direct formation or secretion of adenosine on solid surface is described in literature. Therefore, the observed SERS features appear to be mainly associated with ATP release. The fact that the metabolite largely dominates the SERS signal is probably due to the high concentration of ATP generated outside the bacteria [49]. Moreover, the small size of ATP results in intimate contact with the nanostructures compared to the cell membrane covering large number of nanostructures, leading to reproducible SERS enhancement.

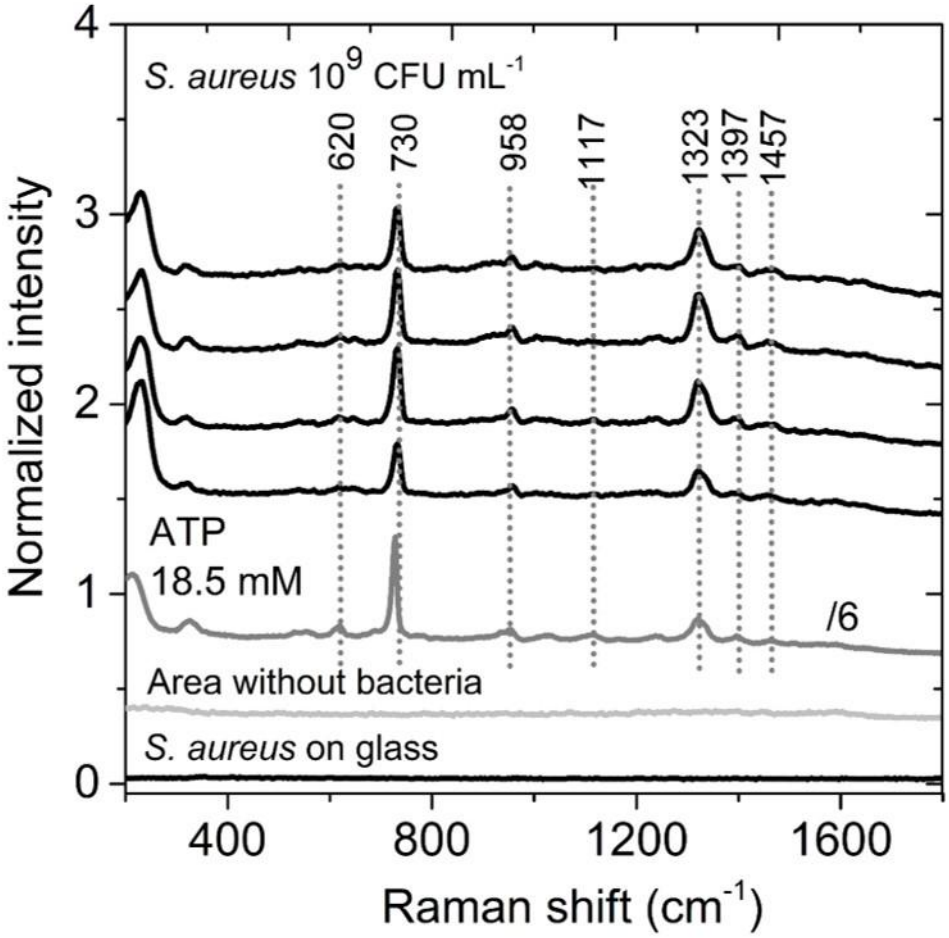

Figure 2. SERS spectra of *S. aureus* ATCC 25923 at 10^9 CFU mL^{-1} on different areas of the glass/Ag film (7 nm) obtained on random places using 633 nm laser excitation at 2.5 mW power, 100× objective, 10 s acquisition time, 1 accumulation. The bottom traces are the SERS spectrum of ATP deposited from a 18.5 mM solution (laser power excitation 0.1 mW), and the featureless spectra of an area of the sample without bacteria and of *S. aureus* directly deposited on a glass slide using the same experimental SERS parameters.

The SERS response of various strains of Gram-negative *E. coli* K12 deposited on the 7 nm-thick film was studied using the same Raman parameters as for *S. aureus* (see Electronic Supplementary Material, **Figure S2-3A**). However, two broad strong-intensity bands located at 1350 and 1560 cm^{-1} are visible which are most likely due to D and G bands of amorphous

carbon, respectively, formed through photo-induced degradation of the lipopolysaccharide layer in Gram-negative bacteria [52]-[53]. Using lower laser power and short Raman acquisition times (see Electronic Supplementary Material, **Figure S2-3Ae**) minimize the carbonization effects and allow the Raman signature of *E. coli* to be recorded. **Figure 3** represents the SERS spectrum of the first strain called *E. coli* Katushka that is genetically modified by the fluorescent protein Katushka. Even under reduced laser power, the reproducibility of *E. coli* Katushka SERS signature, recorded at different places on the substrate, is lower than that obtained for *S. aureus*. This variability is likely to be related to the heterogeneity of the *E. coli* arrangement on the substrate, as compared to the compact carpet of *S. aureus*. However, SERS spectra successively acquired at the same location (see Electronic Supplementary Material, **Figure S2-3B**) do not change even after 9 scans, indicating that no degradation of the sample takes place and underlining the fact that the observed differences originate from the sample itself. Moreover, there is no interference of the growth medium since no SERS response of a non-diluted 2× YT solution is detected and no Raman response is recorded when the bacteria are directly deposited on glass, confirming the SERS effect of the silver nanostructures.

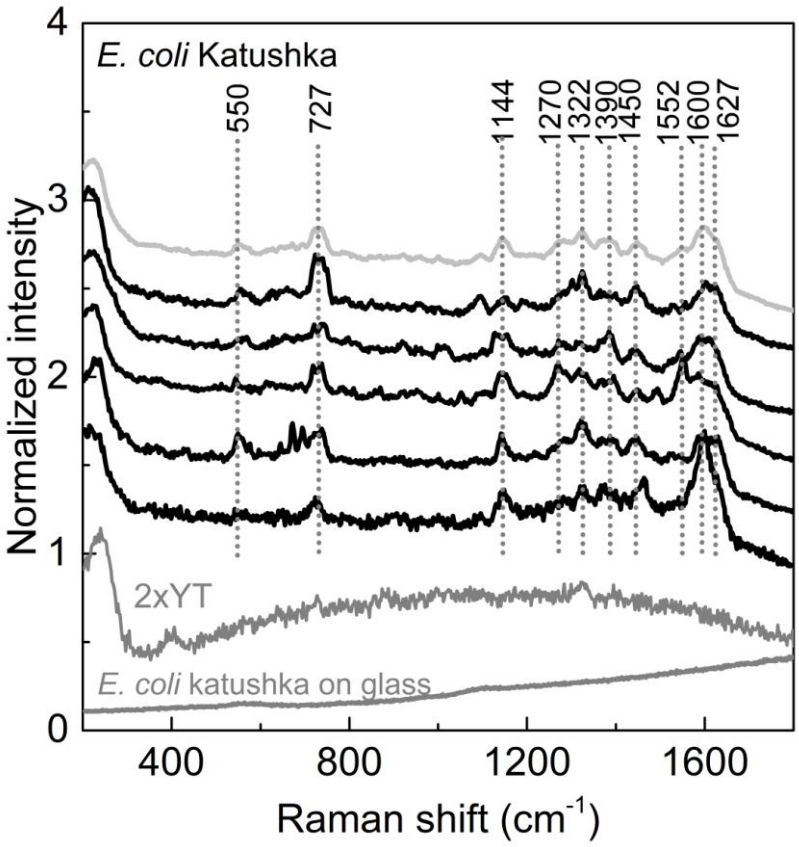

Figure 3. SERS spectra of *E. coli* Katushka (10^{10} CFU mL^{-1}) recorded at different places using 633 nm laser excitation and 100× objective at 0.1 mW power, 10 s acquisition time, 1 accumulation (the top grey spectrum is computed as the average of the 5 spectra of the same frame); As a control, SERS spectra of non-diluted 2× YT solution (bottom grey spectrum) and *E. coli* Katushka directly deposited on glass (bottom grey spectrum) were acquired using the same Raman parameters are presented.

As compared to *S. aureus*, the SERS spectrum of *E. coli* Katushka is also more complex. While the two main bands related to the adenine ring vibrations at 732 and 1322 cm^{-1} are present, there is no correspondence with SERS features of known metabolites or adenine-containing molecules like DNA, RNA or flavin derivatives present in the inner side of the cell wall membrane (riboflavin, flavin adenine dinucleotide FAD) [54]. Several bands related to characteristic vibrations of proteins at 1627 cm^{-1} (amide I), 1552 cm^{-1} (amide II) and 1270 cm^{-}

^{1} (amide III) are observed. The band at 1450 cm^{-1} is ascribed to the deformation modes of C-H from proteins, but also from lipids or saccharides. The band at 1390 cm^{-1} may be attributed to the symmetric stretching mode of carboxylate $\nu_s COO^-$ and at 1154 cm^{-1} to the stretching modes νC-C and νC-N from proteins and/or to νC-C skeleton in lipids. Concerning the vibrations at 550 and 1144 cm^{-1}, their attributions are more complex since they can be associated either with carbohydrate vibrations (deformation and stretching C-O modes, respectively) or with proteins (ν(S-S) and ν(C-C, C-N), respectively) [55],[56],[57]. As reported by Mosier-Ross [7], surface immobilized nanoparticles cannot give information on the inner part of the membrane, i.e. the periplasm made of peptidoglycans since they cannot go through the outer lipopolysaccharide layer of the cell. Since Raman features of adenine derivatives are present, but no secretions or metabolites are observed, we deduce that the SERS features of *E. coli* are mainly due to the proteins from the pili/flagella or outer membrane and to the lipopolysaccharides, which contain adenine part in the lipid layer [9].

We recorded SERS spectra of two other *E. coli* K12 strains devoid of flagella under the same conditions, as previously. From **Figure 4A**, the spectra of *E. coli* JM101TR strain are not perfectly similar when recorded at random places, but their signatures are different from those of *E. coli* Katushka, notably by the disappearance of the three peaks at 550, 1129 and above 1600 cm^{-1}, allowing a discrimination between both strains. The absence of the amide I band might be related to the absence of flagella. In parallel, the δCH_2 of the saturated lipids is seen at 1450 cm^{-1} together with the adenine vibrations at 727 and 1378 cm^{-1}. For the *E. coli* AAEC185(pUT2002) strain, a much higher reproducibility of the SERS spectra is achieved with characteristic vibrations located between 890 and 1130 cm^{-1}, different from those observed for *E. coli* Katushka and JM101TR strains (**Figure 4B**). We note the absence of adenine and amide I vibrations as compared to *E. coli* Katushka, the 880-1130 cm^{-1} spectral

range is richer in bands which may be associated to the C-C and C-O stretchings of the LPS carbohydrates. Finally, the SERS signatures of the last *E. coli* strain called AAEC185(pMMB66) devoid of pili and flagella both reveal a remarquable reproducibility (**Figure 4C**). Adenine vibrations are again visible at 728, 1325, 1397 and 1457 cm^{-1}, suggesting probable secretion of adenine-type metabolites on the Ag substrate. In addition, we observe similar findings with the SERS spectrum of non-treated *E. coli* strains from Lemma *et al*. work [47], notably the two intense bands at 653 and 728 cm^{-1}, suggesting not only adenine-type metabolites but also bacterial genome release. In summary, though some fluctuations are apparent on the SERS spectra, the four strains exhibit four distinguished SERS signatures visible by naked eye, allowing a clear discrimination between the strains.

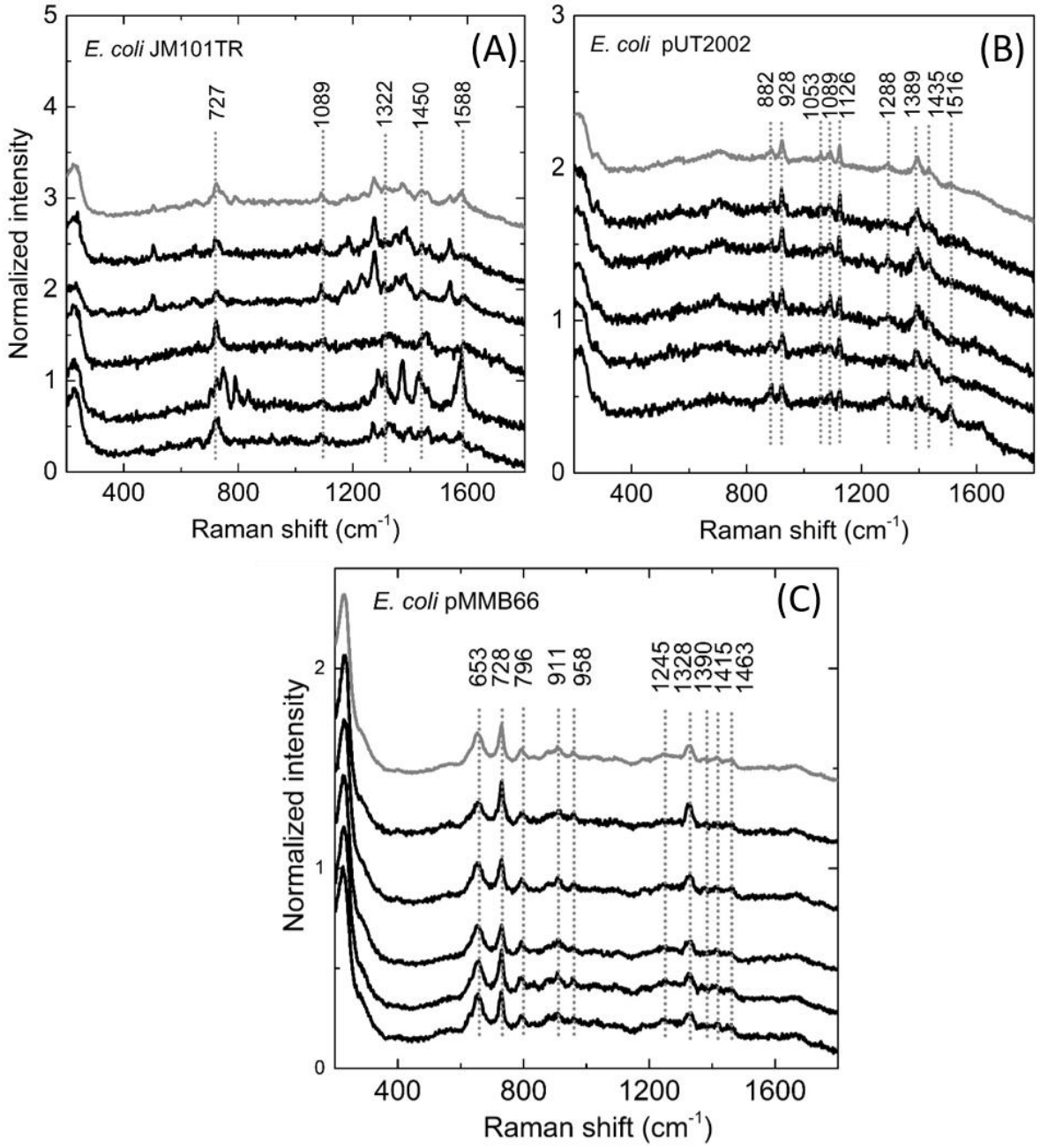

Figure 4. SERS spectra of *E. coli* JM101TR (A), AAEC185(pUT2002) (B), and AAEC185 (pMMB66) (C) strains deposited from 10^{10} CFU mL^{-1} solutions on 7 nm-thick Ag film recorded using 633 nm laser excitation at 0.1 mW, 100× objective, 10 s acquisition time, 1 accumulation. The spectra shown in grey are spectra computed as the average of the 5 spectra of the same frame.

3.2. SERS signature of isolated bacteria

Until now, high bacteria concentrations (deposited from 10^{10} CFU mL^{-1} suspensions) were used for SERS analysis. At such high concentrations, bacteria densely cover the SERS substrate. Decreasing the analysed bacteria concentration leads to the presence of isolated single bacteria on the surface. Such substrates are, therefore, well-suited for the screening of single bacteria cells. We focused on *S. aureus* and *E. coli* JM101TR deposited from 10^4 CFU mL^{-1} solutions on the SERS interface. SEM images were performed after 30 min of contact with the bacteria solution. From **Figure 5**, the lysis of the bacterial cells can be observed in both cases, with an estimation of about 70% of damaged *S. aureus* membrane versus 15% for *E. coli* (based on SEM images). As compared to the densely packed layer of bacteria, low concentrated bacteria seem to be more vulnerable to the bactericidal effect of the silver substrate.

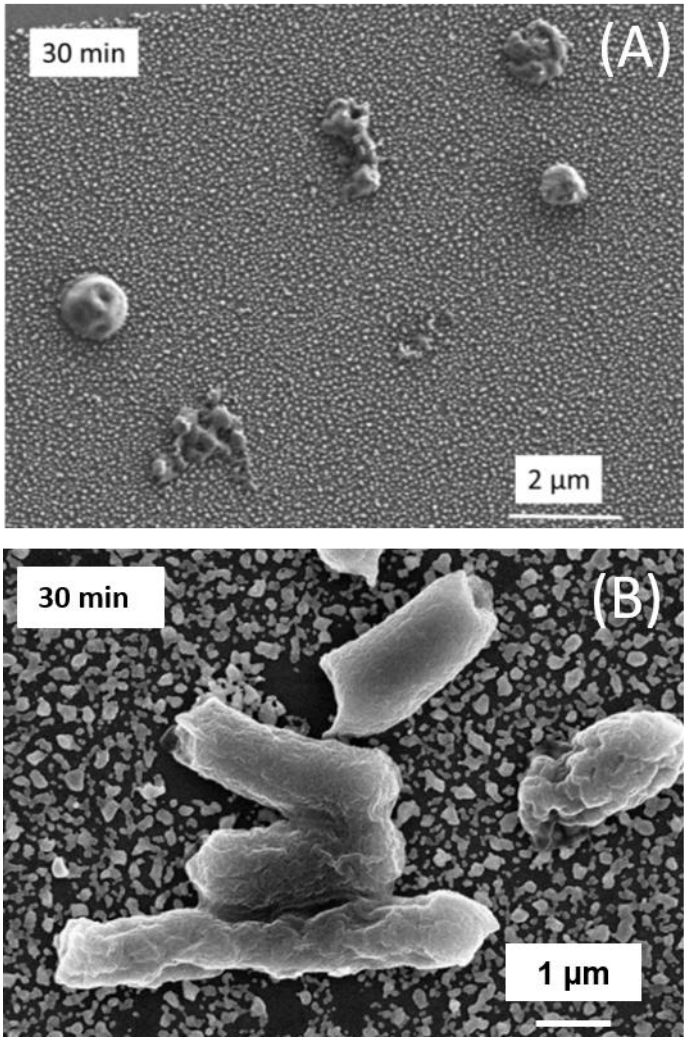

Figure 5. SEM images of *S. aureus* ATCC 43300 (A) and *E. coli* JM101TR (B) deposited from 10^4 CFU mL^{-1} suspension on 7 nm-thick Ag film after 30 min of contact.

Raman measurements were performed at different places around *S. aureus* bacteria islands since they tend to form small clusters, as displayed in the optical image in **Figure S2-4 (**Electronic Supplementary Material). At this scale, no information about the structural integrity of the bacteria is evident. The SERS spectra in **Figure 6A** (recorded using the same acquisition parameters as for the dense layer of *S. aureus*) show more variability even when repeating scans at the same area. The peaks are much less intense, as compared to the spectra in **Figure 2**. Moreover, the ATP signature does not dominate the spectra and new bands

appear, which may be attributed to the bacterial membrane and/or cellular lysis. Concerning *E. coli* JM101TR strain, single isolated bacteria can be obtained, for which two Raman mappings were performed at different places around and on top of a single bacterium. Four representative spectra from each mapping are displayed in **Figure 6B**. The corresponding acquisition points are depicted in the optical images displayed in **Figure S2-5** (see Electronic Supplementary Material) as intersections of the two perpendicular lines. The size of the laser beam (0.4 µm) is drawn as a white circle on the optical image depicted on **Figure S2-5 (**see Electronic Supplementary Material). A third mapping was realized around a group of bacteria, as displayed on **Figure S2-6**, Electronic Supplementary Material.

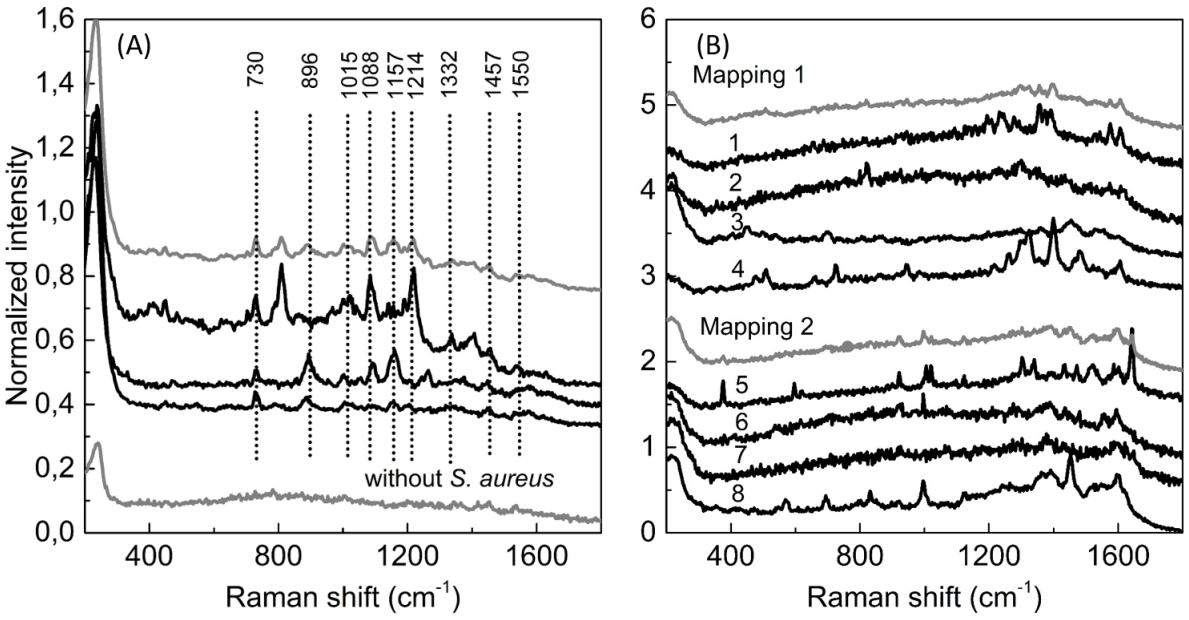

Figure 6. SERS spectra of *S. aureus* (10^4 CFU mL^{-1}) at three different areas recorded at 2.5 mW power, ×100 objective, 10 s acquisition time, 1 accumulation. The top grey spectrum is computed as the average of the 3 spectra of the same frame, the bottom grey spectrum has been recorded at a location free of *S. aureus* (A); Four different spectra extracted from two SERS mappings of a single bacterium *E. coli* JM101TR (10^4 CFU mL^{-1}) at 0.1 mW, 100×

objective, 10 s acquisition time, 1 accumulation (B); the grey spectra are the average of the 4 spectra recorded in each mapping.

The SERS spectra of a single bacterium are not identical and they somewhat differ from those obtained at 10^{10} CFU mL^{-1}. No indication of bacteria lysis (change in shape) can be found in the corresponding microscopy images. Therefore, the variations probably originate from the different environments of the bacterium. The SERS signatures highly depend on the position of the laser beam around the bacterium. For instance, when the laser beam is focused on the top of the bacterium (spectra 2 and 7 in **Figure 8B** or spectrum 11 in **Figure S2-6,** Electronic Supplementary Material), the peak intensities appear much weaker than when the laser beam is located close to the bacteria/Ag interface, suggesting that the SERS signal may arise from the lipopolysaccharides and the pili of the *E. coli* bacterium.

3.3. Statistical analysis of the SERS spectra

To better evaluate the spectral differences at low concentration and compare them with those obtained at higher concentration, the multivariate statistical technique, called principal component analyse (PCA), was used. Although such statistical tools are mainly employed to analyse large datasets, they can be helpful to be applied to a few SERS spectra (less than 5 spectra per strain) as reported in the literature (see for instance [58] and [59]). PCA was performed on all SERS spectra recorded for *S. aureus* and for the four *E. coli* strains presented in **Figures 2, 3, 4** and **6**. The 3D representation shown in **Figure 7** corresponds to the analysis along the first three principal components. This representation straightforwardly allows for distinguishing six clusters: four clusters corresponding to the four distinct strains of *E. co*li bacteria and two distinct clusters for the *S. aureus* strain at high and low surface

concentrations. The spectra corresponding to negative values of PC1 are ascribed to the Katushka strain, those corresponding to positive values of PC1 and positive values of PC2 are assigned to the *E. coli* AAEC185(pMMB66) strain and those corresponding to positive values of PC1 and negative values of PC2 and opposite value of PC3 are due to the *E. coli* AAEC185(pUT2002) and JM101TR strains. Noticeably, in spite of some visual differences, the spectra corresponding to JM101TR bacteria deposited from 10^{10}, 10^{9}, 10^{8} or 10^{4} CFU mL^{-1} suspensions gather in the same cluster (positive value of PC3), confirming that the SERS signals originate from only one type of bacteria. In the case of *S. aureus*, two clusters are obtained, depending on the surface concentration of the bacteria. This observation highlights that the bacteria do not behave similarly at high or low concentration, the Raman spectra bearing signatures from ATP secretion at high concentration and that of bacteria cell wall or cell lysis at low concentration. The high weight of PC1, close to 93%, significates that the corresponding component is the most relevant for discriminating between the various spectra. As a matter of fact, PC1 exhibits a spectral shape similar to that of the Raman spectra recorded for the Katushka strain (more precisely, the opposite of the spectral shape). The high value of the variance ascribed to PC1 therefore reflects the high amplitude variation of the spectra recorded for the Katushka strain. PC2 allows for easily separating the three clusters corresponding to *S. aureus* at low concentration and high concentration and JM101TR strains, at positive and relatively low values of PC1. PC3 permits for distinguishing *E. coli* pMMB66 from *E. coli* AAEC185(pUT2002) and *S. aureus* at low concentration from *E. coli* AAEC185(pMMB66). Apart from the actual differences due to a change of the bacteria behaviour in response to their environment (as those highlighted above for *S. aureus*), spectra appear to exhibit larger variations when probing isolated bacteria rather than dense aggregates. The variability of the SERS response is intrinsic to the very local enhancement of the Raman scattering at some hot spots and is further amplified for the analysis of bacteria,

since the size of the laser spot is smaller than the size of bacteria. When aggregated bacteria cover the Ag nanostructures, the various responses tend to somewhat average, with a locally more uniform environment resulting in more reproducible spectra; this is why spectra recorded at low concentrations are less reproducible and more subject to accidental variations. However, as shown by the PCA, these variations turn out to be not statistically significant, or at least do not take over the variations in the Raman spectra from one strain to another one.

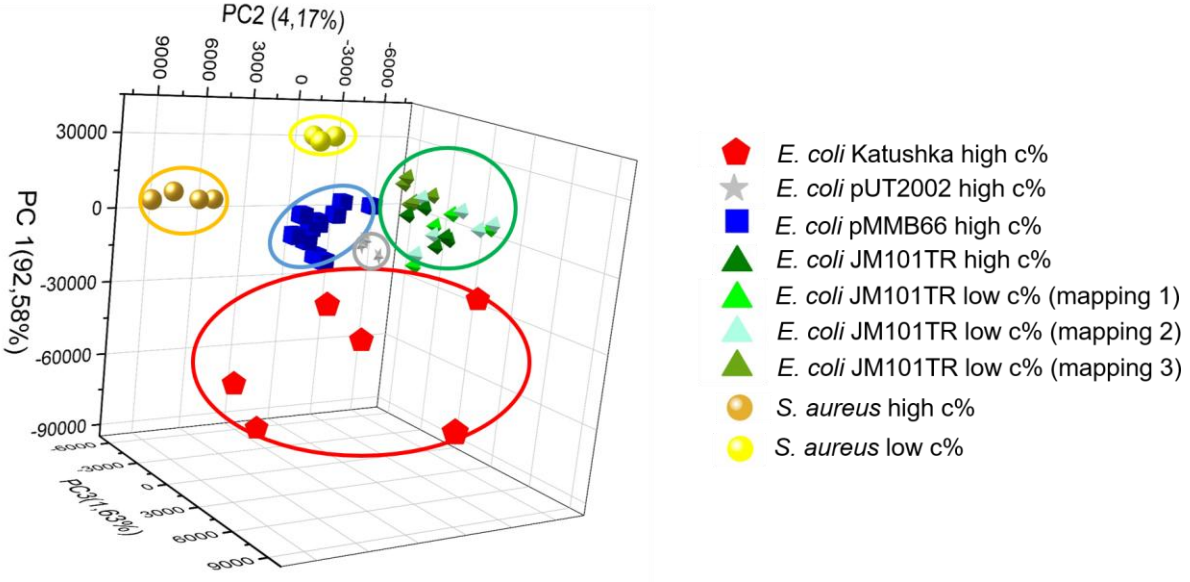

Figure 7. Principal component analysis of SERS spectra recorded for different strains: *E. coli* Katushka (pentagon cluster), JM101TR (triangle cluster), pMMB66 (square cluster), pUT2002 (star cluster) and *S. aureus* (sphere cluster) at high and low concentrations. In the case of *E coli* strain, high concentration refers to 10^{10} CFU.mL^{-1} (carpet of bacteria) and low concentration to 10^{9} - 10^{4} CFU.mL^{-1} (group of bacteria to single bacteria). In the case of *S. aureus*, high concentration refers to 10^{9} CFU.mL^{-1} (carpet) and low concentration to 10^{4} CFU.mL^{-1} (single and small groups of bacteria).

4. Conclusion

The influence of aggregation of *S. aureus* and *E. coli* bacteria on the SERS response was studied using thermally evaporated Ag films. Starting from a dense layer of bacteria, reproducible spectra of *S. aureus* are obtained whereas spectra recorded for *E. coli* appear somewhat more variable. Decreasing the bacteria concentration of the solution deposited on the SERS substrate up to 10^4 CFU mL^{-1} allows for screening a single bacterium; then, more pronounced variations are found from spectra to spectra. We attribute these results to signals arising from different environments surrounding the bacteria together with bactericidal effect of the silver. Thanks to PCA, these differences are shown to be significant and can be rationalized in terms of changes in the integrity of bacteria. Moreover, PCA makes also possible to objectively discriminate between four different strains of *E. coli* thanks to their specific SERS signatures. In the case of *S. aureus*, a different response is observed as a function of the surface concentration of bacteria, giving rise to two distinct clusters in PCA. This separation highlights the secretion of ATP at high concentration, whereas the poor stability of bacteria at low concentration allows for detecting the cell wall signature and/or cell lysis. To conclude, these substrates, in spite of their simple, robust, fast and easy technique of production, meet the challenges for fast single cell analysis of bacteria using SERS. Like many other types of SERS substrates, the obtained spectra may have some specificity associated with the substrate fabrication process, but the substrates allow for obtaining rationalized and meaningful results when the analysis of the spectra includes PCA.

Authors' contributions

The manuscript was written through contributions of all authors. All authors have given approval to the final version of the manuscript. C.-C. A. and A. M. performed the main experiments (preparation of the substrates, *E. coli* growth, SERS measurements). M. P., S. A,

E. J. performed the growth and the SERS spectra of *S. aureus*. L.R. and N.S. did the SEM images of *S. aureus.* A.C.G.-L. and S.S. are thesis supervisors of C.-C. A. with the input of J.B., E. L., F.O. and R.B.

Conflicts of interest/Competing interests

The authors declare no competing financial interests or no personal relationships that could have appeared to influence the work reported in this paper.

Acknowledgments

We gratefully thank the laboratory of biochemistry at Ecole polytechnique, particularly Michel Panvert and Pierre Plateau, for providing us the *E. coli* JM101TR strain, for their help and access to their equipment for the bacteria growth and also for very helpful discussions. We thank Nicolas Barrois from the Center for infection and Immunity of Lille (UMR 8240-INSERM U1090) for help with the SEM analysis. A.C.G.L also thanks Philippe Allongue (LPMC, Ecole polytechnique) for a useful discussion on the manuscript.

Funding information

C.-C. Andrei thanks DGA and Ecole polytechnique for PhD financial support. M. Potara and S. Astilean acknowledge the financial support of a grant of the Romanian Ministry of Research and Innovation, CCCDI – UEFISCDI, project number PN-III-P1-1.2-PCCDI-2017-0010 / 74PCCDI/2018, within PNCDI III. The work is supported financially by the European Union's Horizon 2020 research and innovation program under grant agreement No 690836.

Electronic Supplementary Material

Supplementary data to this article can be found online at …

In **Section 1** is discussed the preparation of silver-based substrates and their optimization for dye probes detection; **Section 2** describes the characterization of bacteria using 7 nm-thick silver films (**Figure S2-1.** Optical images of 7 nm-thick Ag film without and with *S. aureus* and *E. coli* JM101TR; **Figure S2-2.** SERS spectra of *S. aureus* compared with SERS obtained for some biomolecules and metabolites; **Figure S2-3.** SERS spectra of *E. coli* Katushka at different acquisition parameters and at repeated scan on the same location; **Figure S2-4.** Optical image of *S. aureus* deposited at low concentration on 7 nm-thick Ag film; **Figure S2-5.** Locations corresponding to the spectra extracted from two SERS mappings of *E. coli* JM101TR at low concentrations; **Figure S2-6.** Locations corresponding to the spectra extracted from mapping 3 of *E. coli* JM101TR.

References

1. Young KD. The selective value of bacterial shape. Microbiology and Molecular Biology Reviews. 2006;70(3):660-703. doi:10.1128/mmbr.00001-06.
2. Douterelo I, Boxall JB, Deines P, Sekar R, Fish KE, Biggs CA. Methodological approaches for studying the microbial ecology of drinking water distribution systems. Water Research. 2014;65:134-56. doi:10.1016/j.watres.2014.07.008.
3. Cheng JC, Huang CL, Lin CC, Chen CC, Chang YC, Chang SS et al. Rapid detection and identification of clinically important bacteria by high-resolution melting analysis after broad-range ribosomal RNA real-time PCR. Clin Chem. 2006;52(11):1997-2004. doi:10.1373/clinchem.2006.069286.
4. Zhao XH, Li M, Xu ZB. Detection of Foodborne Pathogens by Surface Enhanced Raman Spectroscopy. Front Microbiol. 2018;9:1-13. doi:10.3389/fmicb.2018.01236.
5. Carbonnelle E, Mesquita C, Bille E, Day N, Dauphin B, Beretti JL et al. MALDI-TOF mass spectrometry tools for bacterial identification in clinical microbiology laboratory. Clin Biochem. 2011;44(1):104-9. doi:10.1016/j.clinbiochem.2010.06.017.
6. Stockel S, Kirchhoff J, Neugebauer U, Rosch P, Popp J. The application of Raman spectroscopy for the detection and identification of microorganisms. Journal of Raman Spectroscopy. 2016;47(1):89-109. doi:10.1002/jrs.4844.
7. Mosier-Boss PA. Review on SERS of Bacteria. Biosensors-Basel. 2017;7(4):1-26. doi:10.3390/bios7040051.
8. Efrima S, Bronk BV. Silver colloids impregnating or coating bacteria. J Phys Chem B. 1998;102(31):5947-50. doi:10.1021/jp9813903.
9. Jarvis RM, Goodacre R. Discrimination of bacteria using surface-enhanced Raman spectroscopy. Analytical Chemistry. 2004;76(1):40-7. doi:10.1021/ac034689c.
10. Zhou HB, Yang DT, Ivleva NP, Mircescu NE, Niessner R, Haisch C. SERS Detection of Bacteria in Water by in Situ Coating with Ag Nanoparticles. Analytical Chemistry. 2014;86(3):1525-33. doi:10.1021/ac402935p.

11. Tian ZQ, Ren B, Wu DY. Surface-enhanced Raman scattering: From noble to transition metals and from rough surfaces to ordered nanostructures. J Phys Chem B. 2002;106(37):9463-83. doi:10.1021/jp0257449.
12. Xie XH, Pu HB, Sun DW. Recent advances in nanofabrication techniques for SERS substrates and their applications in food safety analysis. Crit Rev Food Sci Nutr. 2018;58(16):2800-13. doi:10.1080/10408398.2017.1341866.
13. Yu H, Peng Y, Yang Y, Li Z-Y. Plasmon-enhanced light-matter interactions and applications. Npj Computational Materials. 2019;5(45):1-14. doi:10.1038/s41524-019-0184-1.
14. Haynes CL, McFarland AD, Van Duyne RP. Surface-enhanced Raman spectroscopy. Analytical Chemistry. 2005;77(17):338A-46A. doi:10.1021/ac053456d.
15. Sharma B, Frontiera RR, Henry AI, Ringe E, Van Duyne RP. SERS: Materials, applications, and the future. Mater Today. 2012;15(1-2):16-25. doi:10.1016/s1369-7021(12)70017-2.
16. Touahir L, Galopin E, Boukherroub R, Gouget-Laemmel AC, Chazalviel J-N, Ozanam F et al. Localized surface plasmon-enhanced fluorescence spectroscopy for highly-sensitive real-time detection of DNA hybridization. Biosensors & Bioelectronics. 2010;25(12):2579-85. doi:10.1016/j.bios.2010.04.026.
17. Touahir L, Galopin E, Boukherroub R, Gouget-Laemmel AC, Chazalviel J-N, François Ozanam F et al. Plasmonic properties of silver nanostructures coated with an amorphous silicon–carbon alloy and their applications for sensitive sensing of DNA hybridization. Analyst. 2011;136:1859-66 doi:10.1039/c0an01022g.
18. Syu WL, Lin YH, Paliwal A, Wang KS, Liu TY. Highly sensitive and reproducible SERS substrates of bilayer Au and Ag nano-island arrays by thermal evaporation deposition. Surf Coat Technol. 2018;350:823-30. doi:10.1016/j.surfcoat.2018.04.043.
19. Fang SU, Hsu CL, Hsu TC, Juang MY, Liu YC. Surface roughness-correlated SERS effect on Au island-deposited substrate. J Electroanal Chem. 2015;741:127-33. doi:10.1016/j.jelechem.2015.01.028.
20. Chung T, Lee Y, Ahn MS, Lee W, Bae SI, Hwang CSH et al. Nanoislands as plasmonic materials. Nanoscale. 2019;11(18):8651-64. doi:10.1039/c8nr10539a.
21. Rasmussen A, Deckert V. Surface- and tip-enhanced Raman scattering of DNA components. Journal of Raman Spectroscopy. 2006;37(1-3):311-7. doi:10.1002/jrs.1480.
22. Kao P, Malvadkar NA, Cetinkaya M, Wang H, Allara DL, Demirel MC. Surface-enhanced Raman detection on metalized nanostructured poly(p-xylylene) films. Adv Mater. 2008;20(18):3562-5. doi:10.1002/adma.200800936.
23. Olson AP, Spies KB, Browning AC, Soneral PAG, Lindquist NC. Chemically imaging bacteria with super-resolution SERS on ultra-thin silver substrates. Scientific Reports. 2017;7. doi:10.1038/s41598-017-08915-w.
24. Wang KD, Li SM, Petersen M, Wang S, Lu XN. Detection and Characterization of Antibiotic-Resistant Bacteria Using Surface-Enhanced Raman Spectroscopy. Nanomaterials. 2018;8(10):762. doi:10.3390/nano8100762.
25. Kahraman M, Yazici MM, Sahin F, Culha M. Experimental parameters influencing surface-enhanced Raman scattering of bacteria. J Biomed Opt. 2007;12(5). doi:10.1117/1.2798640.
26. Knauer M, Ivleva NP, Niessner R, Haisch C. Optimized Surface-enhanced Raman Scattering (SERS) Colloids for the Characterization of Microorganisms. Anal Sci. 2010;26(7):761-6. doi:10.2116/analsci.26.761.
27. Witkowska E, Nicinski K, Korsak D, Szymborski T, Kaminska A. Sources of variability in SERS spectra of bacteria: comprehensive analysis of interactions between selected bacteria and plasmonic nanostructures. Analytical and Bioanalytical Chemistry. 2019;411(10):2001-17. doi:10.1007/s00216-019-01609-4.
28. Qiu L, Wang WQ, Zhang AW, Zhang NN, Lemma T, Ge HH et al. Core-Shell Nanorod Columnar Array Combined with Gold Nanoplate-Nanosphere Assemblies Enable Powerful In Situ SERS

Detection of Bacteria. Acs Applied Materials & Interfaces. 2016;8(37):24394-403. doi:10.1021/acsami.6b06674.
29. Kaminska A, Witkowska E, Kowalska A, Skoczynska A, Ronkiewicz P, Szymborski T et al. Rapid detection and identification of bacterial meningitis pathogens in ex vivo clinical samples by SERS method and principal component analysis. Analytical Methods. 2016;8(22):4521-9. doi:10.1039/c6ay01018k.
30. Guerrini L, Graham D. Molecularly-mediated assemblies of plasmonic nanoparticles for Surface-Enhanced Raman Spectroscopy applications. Chemical Society Reviews. 2012;41(21):7085-107. doi:10.1039/c2cs35118h.
31. Pilot R, Signorini R, Durante C, Orian L, Bhamidipati M, Fabris L. A Review on Surface-Enhanced Raman Scattering. Biosensors-Basel. 2019;9(2). doi:10.3390/bios9020057.
32. Mechulam Y, Blanquet S, Fayat G. Dual level control of the Escherichia coli pheST-himA operon expression- tRNA(phe)-dependent attenuation and transciptional operator repressor control by himA and the SOS network J Mol Biol. 1987;197(3):453-70. doi:10.1016/0022-2836(87)90558-4.
33. Hirel PH, Leveque F, Mellot P, Dardel F, Panvert M, Mechulam Y et al. Genetic engineering of methionyl-transfert RNA synthetase: invitro regeneration of an active synthetase by proteolytic cleavage of a methionyl transfert RNA synthetase-β-galactosidase chimeric protein Biochimie. 1988;70(6):773-82. doi:10.1016/0300-9084(88)90107-1.
34. Yan X, Sivignon A, Yamakawa N, Crepet A, Travelet C, Borsali R et al. Glycopolymers as Antiadhesives of E. coil Strains Inducing Inflammatory Bowel Diseases. Biomacromolecules. 2015;16(6):1827-36. doi:10.1021/acs.biomac.5b00413.
35. Blomfield IC, McClain MS, Eisenstein BI. Type-1 fimbriae mutants of Escherichia coli K12 - characterization of recognized afimbriate strains and construction of new fim deletion mutants. Mol Microbiol. 1991;5(6):1439-45. doi:10.1111/j.1365-2958.1991.tb00790.x.
36. Wilson WW, Wade MM, Holman SC, Champlin FR. Status of methods for assessing bacterial cell surface charge properties based on zeta potential measurements. Journal of Microbiological Methods. 2001;43(3):153-64. doi:10.1016/s0167-7012(00)00224-4.
37. Ahern AM, Garrell RL. In situ photoreduced silver nitrate as a substrate for Surface-enhnaced Raman spectroscopy Analytical Chemistry. 1987;59(23):2813-6. doi:10.1021/ac00150a020.
38. Kovacs GJ, Loutfy RO, Vincett PS, Jennings C, Aroca R. Distance dependence of SERS enhancement factor from Langmuir-Blodgett monolayers on metal island films -evidence for the electromagnetism mechanism. Langmuir. 1986;2(6):689-94. doi:10.1021/la00072a001.
39. Zeiri L, Bronk BV, Shabtai Y, Czege J, Efrima S. Silver metal induced surface enhanced Raman of bacteria. Colloid Surf A-Physicochem Eng Asp. 2002;208(1-3):357-62. doi:10.1016/s0927-7757(02)00162-0.
40. Naja G, Bouvrette P, Hrapovic S, Luong JHT. Raman-based detection of bacteria using silver nanoparticles conjugated with antibodies. Analyst. 2007;132(7):679-86. doi:10.1039/b701160a.
41. Giese B, McNaughton D. Surface-enhanced Raman spectroscopic and density functional theory study of adenine adsorption to silver surfaces. J Phys Chem B. 2002;106(1):101-12. doi:10.1021/jp010789f.
42. Premasiri WR, Lee JC, Sauer-Budge A, Theberge R, Costello CE, Ziegler LD. The biochemical origins of the surface-enhanced Raman spectra of bacteria: a metabolomics profiling by SERS. Analytical and Bioanalytical Chemistry. 2016;408(17):4631-47. doi:10.1007/s00216-016-9540-x.
43. Premasiri WR, Gebregziabher Y, Ziegler LD. On the Difference Between Surface-Enhanced Raman Scattering (SERS) Spectra of Cell Growth Media and Whole Bacterial Cells. Applied Spectroscopy. 2011;65(5):493-9. doi:10.1366/10-06173.
44. Rimai L, Cole T, Parsons JL, Hickmott JT, Carew EB. Studies of Raman spectra of water solutions of adeosine tri- di- and monophosphate and some related compounds Biophysical Journal. 1969;9(3):320-9. doi:10.1016/s0006-3495(69)86389-7.

45. Wu C-Y, Lo W-Y, Chiu C-R, Yang T-S. Surface enhanced Raman spectra of oligonucleotides induced by spermine. Journal of Raman Spectroscopy. 2006;37(8):799-807. doi:10.1002/jrs.1506.
46. Prescott B, Steinmetz W, Thomas GJ. Raman spectral studies of nucleic acids. 23. Characterization of DNA by laser Raman spectroscopy Biopolymers. 1984;23(2):235-56. doi:10.1002/bip.360230206.
47. Lemma T, Saliniemi A, Hynninen V, Hytonen VP, Toppari JJ. SERS detection of cell surface and intracellular components of microorganisms using nano-aggregated Ag substrate. Vib Spectrosc. 2016;83:36-45. doi:10.1016/j.vibspec.2016.01.006.
48. Mempin R, Tran H, Chen CN, Gong H, Ho KK, Lu SW. Release of extracellular ATP by bacteria during growth. Bmc Microbiology. 2013;13. doi:10.1186/1471-2180-13-301.
49. Cui L, Zhang YJ, Huang WE, Zhang BF, Martin FL, Li JY et al. Surface-Enhanced Raman Spectroscopy for Identification of Heavy Metal Arsenic(V)-Mediated Enhancing Effect on Antibiotic Resistance. Analytical Chemistry. 2016;88(6):3164-70. doi:10.1021/acs.analchem.5b04490.
50. Ivanova EP, Alexeeva YV, Pham DK, Wright JP, Nicolau DV. ATP level variations in heterotrophic bacteria during attachment on hydrophilic and hydrophobic surfaces. Int Microbiol. 2006;9(1):37-46.
51. Tuson HH, Weibel DB. Bacteria-surface interactions. Soft Matter. 2013;9(17):4368-80. doi:10.1039/c3sm27705d.
52. Hong SH, Winter J. Micro-Raman spectroscopy on a-C : H nanoparticles. Journal of Applied Physics. 2005;98(12):124304. doi:10.1063/1.2142078.
53. Gromov DG, Dubkov SV, Savitskiy AI, Shaman YP, Polokhin AA, Belogorokhov IA et al. Optimization of nanostructures based on Au, Ag, Au-Ag nanoparticles formed by thermal evaporation in vacuum for SERS applications. Applied Surface Science. 2019;489:701-7. doi:10.1016/j.apsusc.2019.05.286.
54. Efrima S, Zeiri L. Understanding SERS of bacteria. Journal of Raman Spectroscopy. 2009;40(3):277-88. doi:10.1002/jrs.2121.
55. Zhou HB, Yang DT, Ivleva NP, Mircescu NE, Schubert S, Niessner R et al. Label-Free in Situ Discrimination of Live and Dead Bacteria by Surface-Enhanced Raman Scattering. Analytical Chemistry. 2015;87(13):6553-61. doi:10.1021/acs.analchem.5b01271.
56. Notingher I. Raman Spectroscopy cell-based Biosensors. Sensors. 2007;7(8):1343-58. doi:10.3390/s7081343.
57. Lu XN, Samuelson DR, Xu YH, Zhang HW, Wang S, Rasco BA et al. Detecting and Tracking Nosocomial Methicillin-Resistant Staphylococcus aureus Using a Microfluidic SERS Biosensor. Analytical Chemistry. 2013;85(4):2320-7. doi:10.1021/ac303279u.
58. Avci E, Kaya NS, Ucankus G, Culha M. Discrimination of urinary tract infection pathogens by means of their growth profiles using surface enhanced Raman scattering. Analytical and Bioanalytical Chemistry. 2015;407(27):8233-41. doi:10.1007/s00216-015-8950-5.
59. Liao WL, Lin QY, Xie SC, He Y, Tian YH, Duan YX. A novel strategy for rapid detection of bacteria in water by the combination of three-dimensional surface-enhanced Raman scattering (3D SERS) and laser induced breakdown spectroscopy (LIBS). Analytica Chimica Acta. 2018;1043:64-71. doi:10.1016/j.aca.2018.06.058.

Graphical abstract